IOSR Journal of Applied Geology and Geophysics (IOSR-JAGG)
e-ISSN: 2321–0990, p-ISSN: 2321–0982. Volume 14, Issue 3 Ser. 1 (May – June 2026), PP 23-33
www.iosrjournals.org

Depth and Edge Delineation of Hydrothermal Mineral bearing Structures based on Magnetic data: A Case Study of Wagusu Gold Prospect, Kenya

Warega J.A* [1], K'Orowe Maurice [2], Githiri John [2], Munyithya James [2]
[1] *Jomo Kenyatta University of Agriculture and Technology, Physics Department, Nairobi, Kenya*
[2] *Jomo Kenyatta University of Agriculture and Technology, Physics Department, Nairobi, Kenya*
Corresponding Author: WEREGA Joseph Ayieta

Abstract
Wagusu magnetic data set was analyzed to delineate crustal signatures that could favor exploration of economic minerals. Depths and edges for litho-structural anomalies were detected by using high resolution methods of Analytic Signal, Tilt angle Derivative and Power spectral analysis, in Oasis Montaj software. Magnetic anomaly distribution in the area ranged between 931.1 nT and 1020.2 nT. The RTP maps revealed variation of causative structures striking in North East-SouthWest direction. The overlain analytic signal revealed maximum signal values over the anomalies covering an estimated area of 4,000,000 m^2. These high amplitude signals are associated with mafic basement rocks uplifted to moderate near the surface which could be hosting minerals and their mineral associations such as banded-iron gold formation. Low magnetic amplitude has been suggested to indicate a acidic type of granitoid that intrudes the area, a sign of loss of magnetic property of magnetite minerals to hematite minerals showing low magnetic response due to hydrothermal fluid flow through lineaments. Tilt angle derivative revealed high magnetic intensity gradient between the magnetic anomaly of high susceptibility and the magnetic anomaly of low susceptibility where shear zones and faults are universally developed along these contrasting zones and along thin incompetent structural units. Power spectral analysis suggested depth to magnetic anomalies between 2150 m for shallow and 4000 m for deep sources. The results, therefore suggested intense basement rocks deformation with tectonic framework supporting mineralization.
Keywords*: Magnetic data; Wagusu; Power Spectral Analysis; Tilt angle Derivative; Analytic Signal; Depth; Edge; Mineralization; Kenya.*

Date of Submission: 25-05-2026 Date of Acceptance: 06-06-2026

I. Introduction

Magnetic mapping is a geophysical method that is applied to locate and mirror subsurface targets. Magnetic anomaly deduction is a complex process due to acquisition, positioning error, multiple sources superposition, and the occurrence of geologic and cultural noise. Therefore, magnetic intensity maps, and other statistical representations that are derived from field data are affected by noises that require application of different edge detection filters for potential field anomalies in order to visualize different features in magnetic intensity maps and hence subtle information can be deduced. In this regard there are various filters for edge detection, like derivative-based filters and local phase filters that apply a change in quantity over magnetic anomalies. Vertical and horizontal derivatives of potential field data are both useful; horizontal derivative visualizes edges, whereas vertical derivative narrows anomaly width, thereby locating causative bodies more accurately. It is also possible to combine both vertical and horizontal derivatives of the magnetic field to achieve an analytic signal that is independent from body magnetization direction in 2D case. The local phase filters like tilt angle derivative is commonly used majorly for edge detection of anomalies. In practice, it is being used because it does not depend on geologic parameters like magnetic susceptibility, angles of deflection, permanent magnetization, and inclination that can affect results. In this regard, calculation for tilt angles values of horizontal and vertical derivative of the magnetic anomalies was done on a 50m-5000m band pass filter and up continued data. Since Wagusu area lies in low magnetic susceptibility latitude, reduction to pole procedure was first applied on magnetic data in Oasis Montaj software before tilt angle derivative was done to improve visualization of causative anomalies. For limiting depth of magnetic causative anomalies, power spectral analysis technique is commonly used.

1.1 Study Area

Wagusu, the study area is situated in southern region of Bondo in Siaya-County Kenya. It borders West Sakwa ward in the north east, Victoria Lake in the south and South West Sakwa ward in the north west. It lies within the Nyanza greenstone belt to the west of the Kavirondo (Rift valley), an arm of the East-Africa system and forms about a quarter of the western terrain of the Nyanza gold belt (Shackleton, 1951). The Nyanza greenstone complex is part of the greenstone complexes of Western Kenya which are associated with the Tanzania's, Craton (Borg *et al*., 1990).

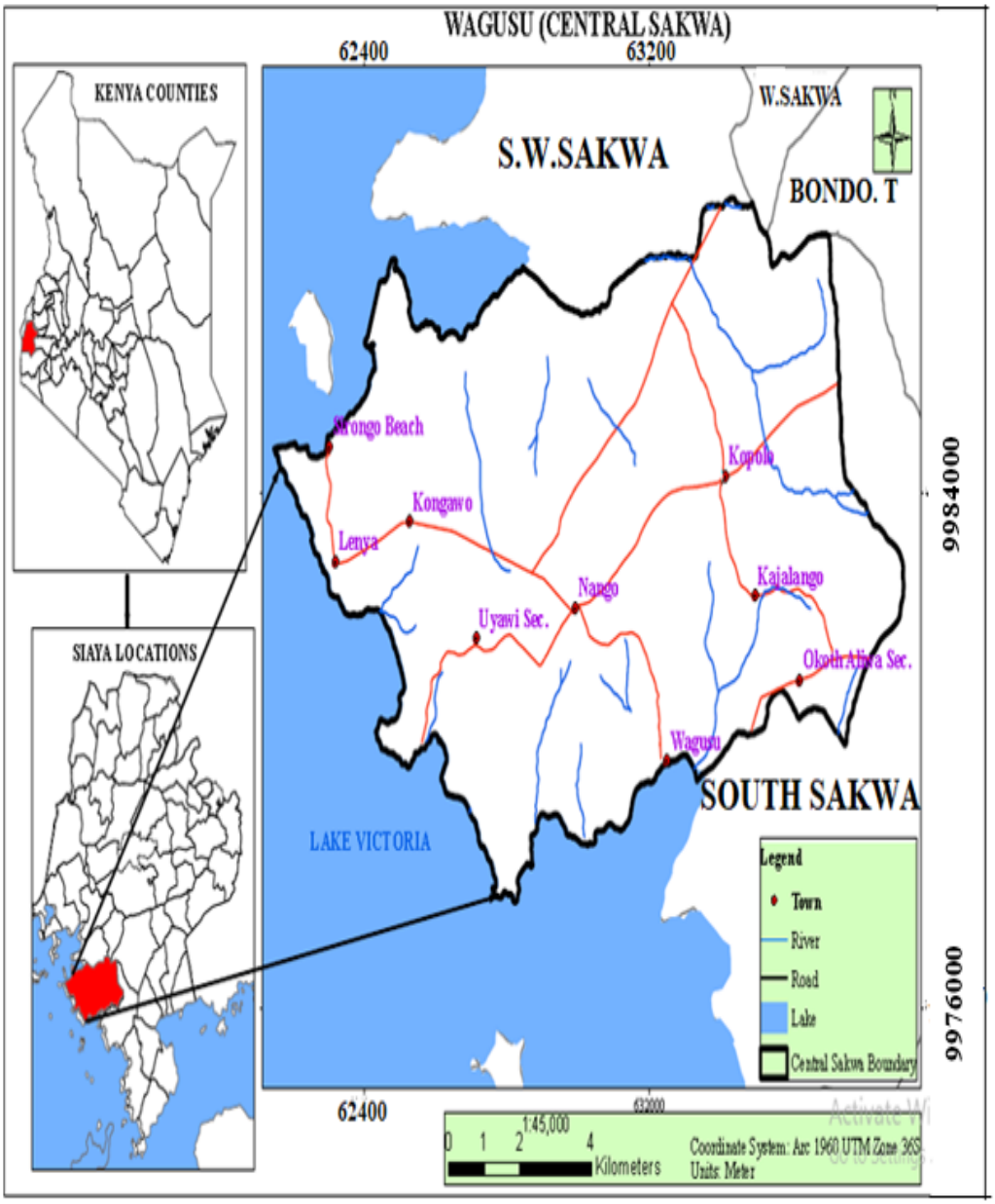

Figure 1.0: Location of the study area (Warega et al)

II. Magnetic Data

Magnetic data sets were collected from a total of 446 stations profiled over the study area. Two G-856 model of proton precession magnetometers, were used. One magnetometer was moved periodically to stations to collect data while the other was positioned at the base station taking readings after every 10 minutes throughout the day for diurnal variation correction. Readings for easting, northing, magnetic and occupation time were recorded at each station. All variations in total field magnetic intensity that came from magnetic intensity of the underlying rocks that included diurnal variation and geomagnetic field were removed from the field measured

magnetic data to get residual magnetic anomaly data. Similarly, International Geomagnetic Reference Field was computed by IGRF calculator embedded in Oasis Montaj software and removed before the residual data was finally analyzed and interpreted. This process is known as magnetic data correction.

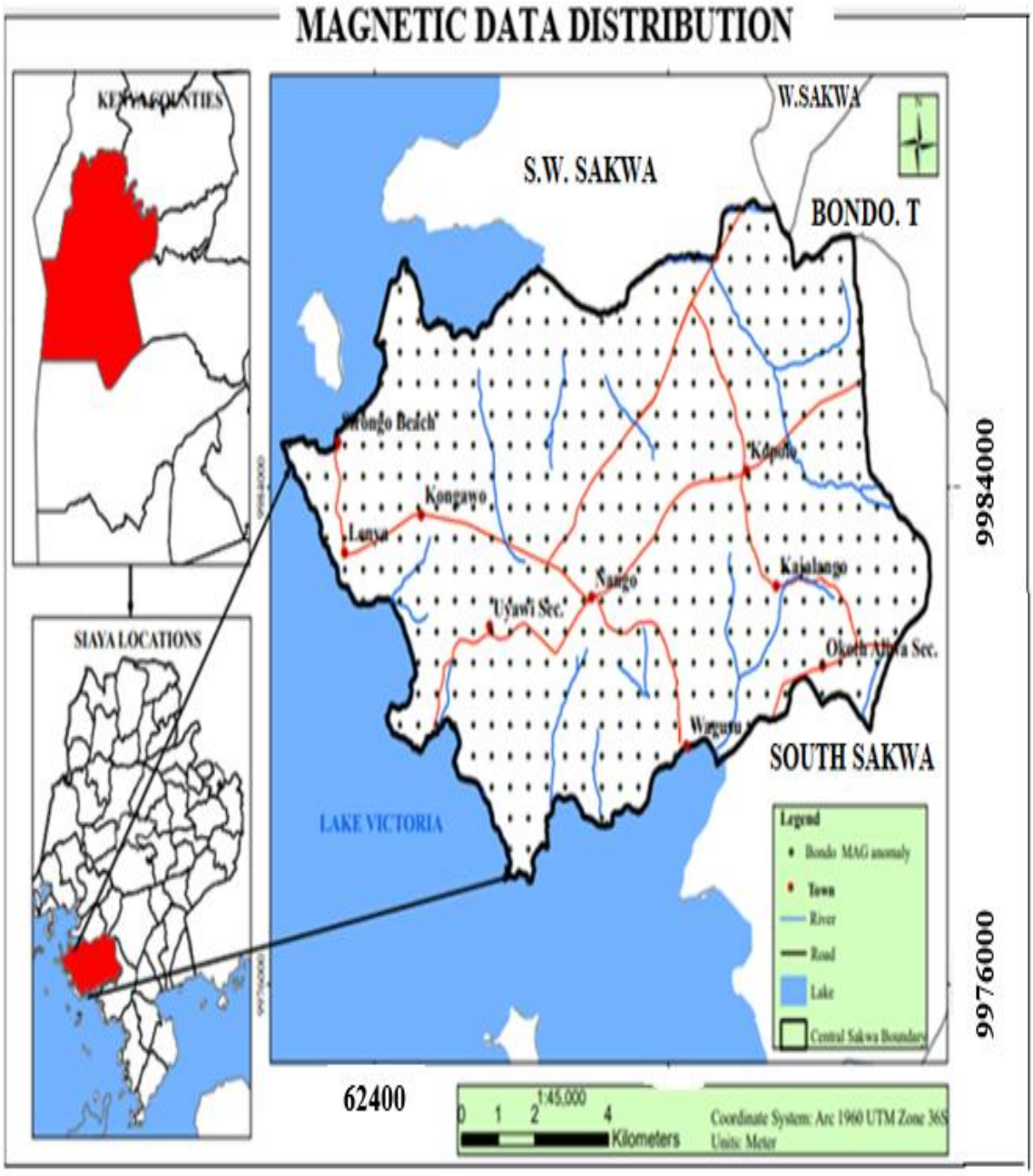

Figure 2: Magnetic stations distribution over Wagusu

2.1 Magnetic anomaly map

Magnetic anomaly data that resulted after diurnal and geomagnetic reductions were done on the raw magnetic data. Figure 2.1 displays a magnetic anomaly map for Wagusu, with purple and orange colors on color bar representing high amplitude magnetic susceptibility up to 1020.2 nT while blue and green colors showing low amplitude magnetic susceptibility up to 823.9 nT. High and low amplitude magnetic susceptibilities are also evident in the central, southern and eastern regions with most high peaking at west of Wagusu, Uyawi Sec, Kajalango and Okoth Aliwa sec areas. Their magnetic magnitude points to high magnetic anomalies buried at probably shallow depths. These could possibly be basic igneous intrusive rocks or magnetite and Pyrrhotite contents imaged at reduced temperature. Temperature and depth of Earth's crust are linearly dependent and affect magnetization of rocks. Crustal temperature increases as depth which subsequently affect magnetic susceptibility

of rocks. At shallow depths, magnetization of magnetite or Pyrrhotite contents tend to increase due to reducing temperature (Kearey et al., 2002). The orange color anomalies peaking at 931.1 nT in some parts of Central and Southern regions of Uyawi Sec, Kajalango and Wagusu reveal high magnetic amplitude, probably of basic igneous intrusion like Basalt or Magnetite and Pyrrhotite contents buried at some depths with their magnetization ability reduced by possibly high temperature at depth. To the northern western region low magnetic amplitude dominate with few packets of high amplitude magnetic susceptibility being witnessed. Sirongo Beach and East wards, predict a potential low magnetic amplitude anomaly or it is a deeply seated magnetite mass beyond the sensitivity of the magnetometer sitting on igneous rock rich region. This ambiguity could be eliminated by filtering the data to obtain residual magnetic data for further analysis and interpretation of the region. It is suggested that magnetic anomaly map of Wagusu reveals good response to magnetic susceptibilities by probably basic igneous intrusions or magnetite and Pyrrhotite contents at shallow depths. This shows that there was a magmatic activity that brought these masses near the surface or their top depths were increased by erosion over millions of years. It further indicates that these masses gained their magnetization during cooling process. They could possibly represent gold bored in banded iron formation of the greenstone belt.

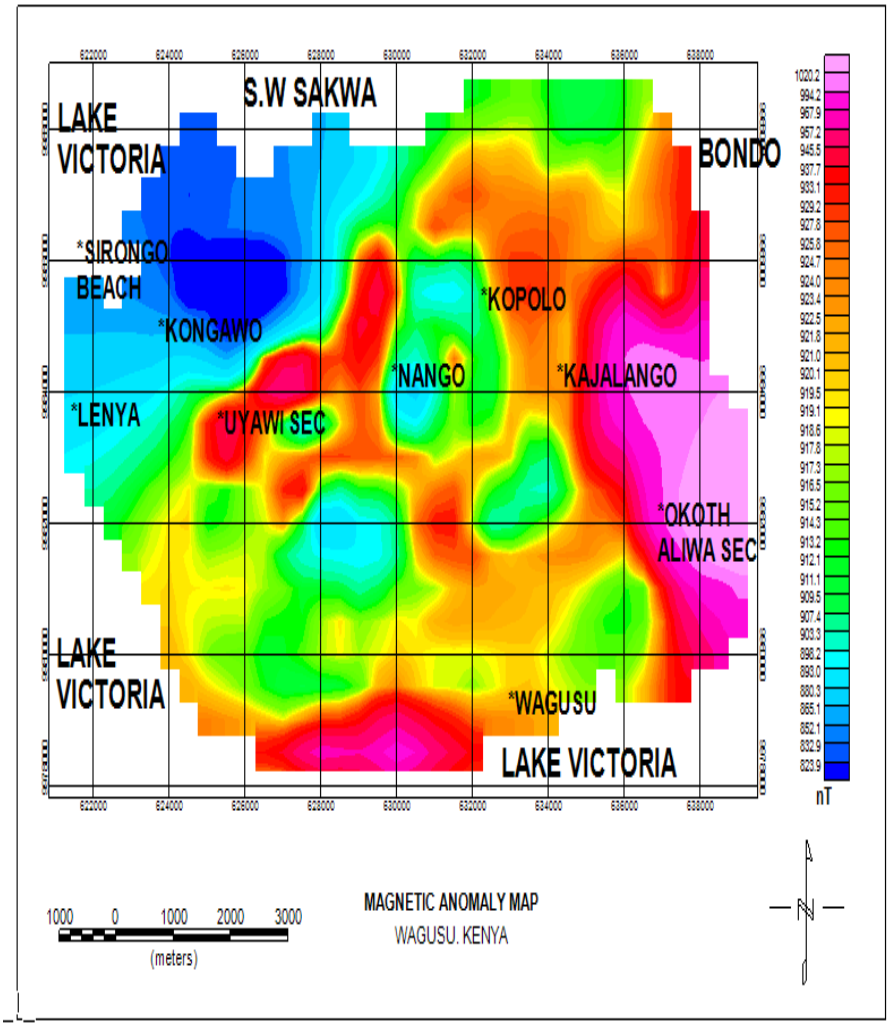

Figure 2.1: Magnetic Anomaly map

2.2 Magnetic residual anomaly (RTP) map

Figure 2.2 represents a residual magnetic Reduce To Pole (RTP) anomaly map filtered between a band pass of 50m and 5000m deep. It resulted after diurnal and geomagnetic reductions were made on magnetic field data and further reduced to magnetic north pole. Residual magnetic anomaly map displayed emanated from the effect of geomagnetic field due to the presence of materials between band pass of 50m and 5000m in depth and as if it were measured at the magnetic north pole where the field symmetry is vertical about its causative anomaly. Filter for RTP was applied to remove this asymmetric of magnetic anomalies since the study area lies in low latitude region This band pass depth range was carefully chosen since gold deposits occurrence in greenstone belts do not go beyond 5000m deep. The figure 2.2 depicts distribution of high-resolution magnetic signatures of high

susceptibility magnetic anomaly shaded color pink or red on the color bar and low magnetic susceptible anomaly coded color green or blue (Fig. 2.2). From the magnetic (RTP) residual anomaly map, high magnetic anomalous zones in an igneous dominated regions like Uyawi secondary, Kongawo, Lenya and Sirongo beach are related to basic intrusive like Basalt bearing magnetite or pyrrhotite minerals. In regions geologically dominated by metamorphic rocks, high magnetic signatures like Nango and Wagusu regions are correlated to magnetite minerals which were resorbed due to relatively low pressure of oxygen where iron and oxygen are incorporated. Moderate to high magnetic anomalous contact zones. The Figure 2.2 exhibits hydrothermal demagnetization of magnetite minerals from basic to intermediate to acidic through faults or fractures or contact boundaries by either possibly elevated temperature or change of geological structure of rocks from basicity to acidity. The phenomenon of this kind correlates to the type of Paleoproterozoic Birimian belt granitoids. Clear boundaries between magnetic susceptibility lows and magnetic susceptibility highs as witnessed from the Figure 2.2 are interpreted possibly to be contact zones laying between these magnetic contrasting competencies. Mineral deposits are commonly found at the contact zones of these contrasting competencies. They probably reflect deep faults or contact zones. Since gold deposits are found near or along these contact zones, we believe that these contact zones control gold mineralization in Wagusu, the study area. It was for these suspected mineralization zones that bore the idea of deploying edge detection and depth estimation techniques for visual enhancement of these anomalies.

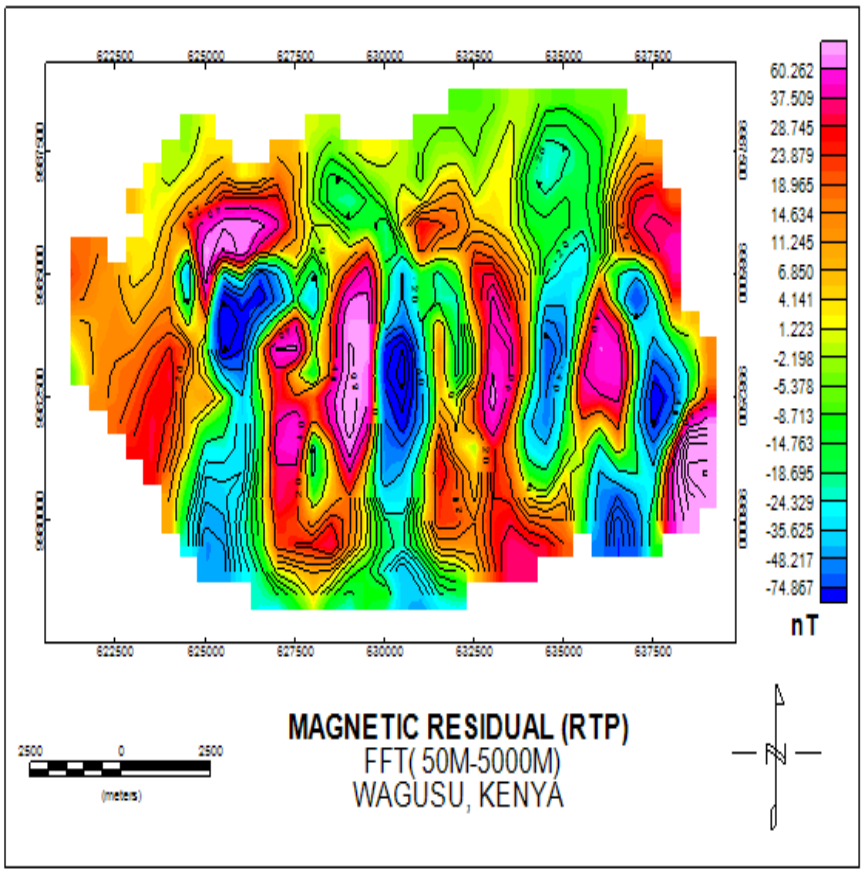

Figure 2.2: Residual Magnetic (RTP) Anomaly map

III. Edge detection and Depth estimation for Magnetic data

Magnetic anomalies derived from potential field data usually decays fast with distance from the source. This property may be made use of by various techniques for depth and edge detection. The technique to be used for anomalies is high visualization dependant hence the choice for high resolution techniques that include analytic signal, power spectral analysis and tilt angle derivative.

3.1 Analytic Signal (AS) of Gravity data

Analytic Signal is a powerful technique for delineating edges of shallow magnetic sources owing to the fact that the amplitude of the analytical signal peaks over the gravity sources (Cooper, 2009). It is defined as the square root of sum of the squares of the derivatives of x and y given by Eq. (1) for a 2D case.

$$|AS| = \sqrt{(\frac{\partial F}{\partial x})^2 + (\frac{\partial F}{\partial y})^2} \quad (1)$$

where F represents magnetic field

For this study, analytic signal for gridded magnetic data was done after passing through a 50m-5000m band filter then reduced to pole in Oasis Montaj software. Calculation for x, y and z derivatives was performed and their respective analytic signal grid maps were generated. Maximum amplitude of analytic signal was interpreted to be the edges of magnetic structures. Figure 3.1, displays analytic signal of the residual magnetic map. It reveals some peaks over locations where magnetite and pyrrhotite materials as well as their associates have been deposited with the most visible ones are to north west of Kongawo and Nango - central parts of the map. The maximum signal values over the anomalies cover an estimated area of 4,000,000 m^2. These high amplitude signals are associated with basic basement rocks uplifted to moderate near the surface which could be hosting minerals and their mineral associations such as banded-iron gold formation. A change in the magnetic susceptibility to low would indicate acidic belt granitoid type that intrudes the area, a manifestation of loss of magnetic property in magnetite minerals to become hematite minerals having low magnetic susceptibility due to hydrothermal fluid flow through lineaments.

Furthermore, the edges along the magnetic anomalies are definite enough to also define faults and shear zones as well as the sizes of basement structures. The basement complex in the study area could have been defined by different tectonic trends as can be observed from the RTP anomaly map (Fig.3.1).

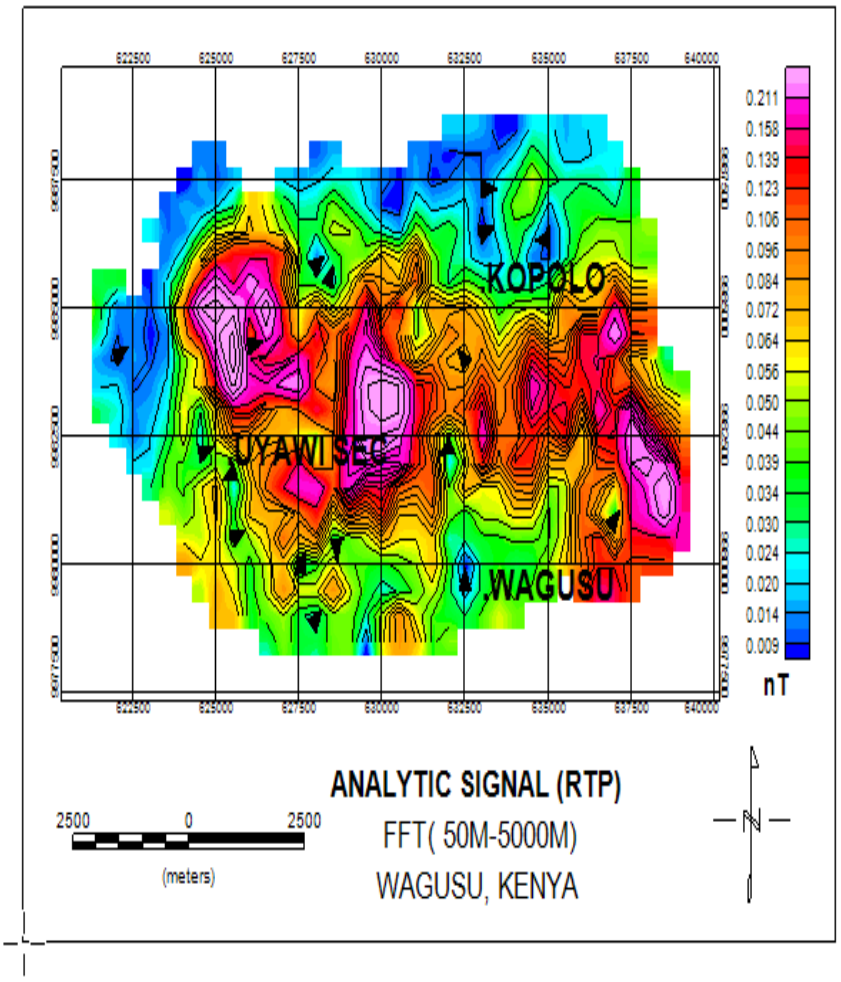

Figure 3.1: Analytic Signal map for residual RTP Magnetic data

3.2 Tilt angle Derivative of Magnetic data

Tilt angle derivative is commonly used for edge visualization and depth estimation of gravity and magnetic anomalies. In practice, it is used since it does not depend on geomagnetic field properties such as magnetic susceptibility, permanent magnetization and inclination that can impact on outcomes. It produces positive values directly above the sources; negative values away from the sources and a zero value over or close to the source edges and therefore can be used to trace the edges (Miller and Singh, 1994).

The tilt angle filter is given by Eq. (2).

$$\theta = tan - 1\left(\frac{VDR}{THDR}\right) \quad (2)$$

For this study, a band pass filter of 50 m-5000 m was used to calculate tilt angles of vertical and horizontal derivative of the magnetic field, up continued then reduced to pole in Oasis Montaj software. The resulted gridded data was used to draw an anomaly map, figure 3.2. The figure 3.2 reveals high magnetic amplitudes sandwiched between low magnetic amplitudes of causative anomalies in a N-S orientation. The red or pink color values on the color bar correspond to the high magnetic amplitude of the anomalies and their estimated top depths calculated by the tilt angle derivative. The figure 3.2 displays depths of the anomalies that range from 216 m to 1271m. Negative sign attached to the values on the color bar also signifies depth. The negative and positive signs of depth are as a result of negative and positive angles observed at tilt angle derivatives. The high magnetic amplitudes delineate causative anomalies at an average top depth of 500m and about 1200m in thickness running a subsurface distance of about 7500 m long. These causative anomalies are mapped over igneous and metamorphic rocks dominant regions. The anomalies could possibly basic or ultra basic intrusive units containing magnetite or pyrrhotite or banded iron formation minerals in the metamorphic and unconsolidated rocks regions. The map also reveals contacts of causative anomalies. The contacts mapped in the study area are indicated by high magnetic intensity gradient between magnetic amplitude anomaly highs and magnetic amplitude anomaly lows. Shear zones and faults are universally developed along these contrasting magnetic competencies. Within these contacts and incompetent rocks; mineral deposits sit at these points of structural weaknesses. Competent rocks being enclosed in less competent favor fracturing and veining in the study area Figure 3.2 that provide suitable home for quartz vein gold.

Common mineral associations of this kind include differentiated dolerite sills, tholeiitic basalts and banded iron formation. These fault lines or fractures or vein or contact zones could be the path ways for hydrothermal mineral deposits such as gold being carried to near surface.

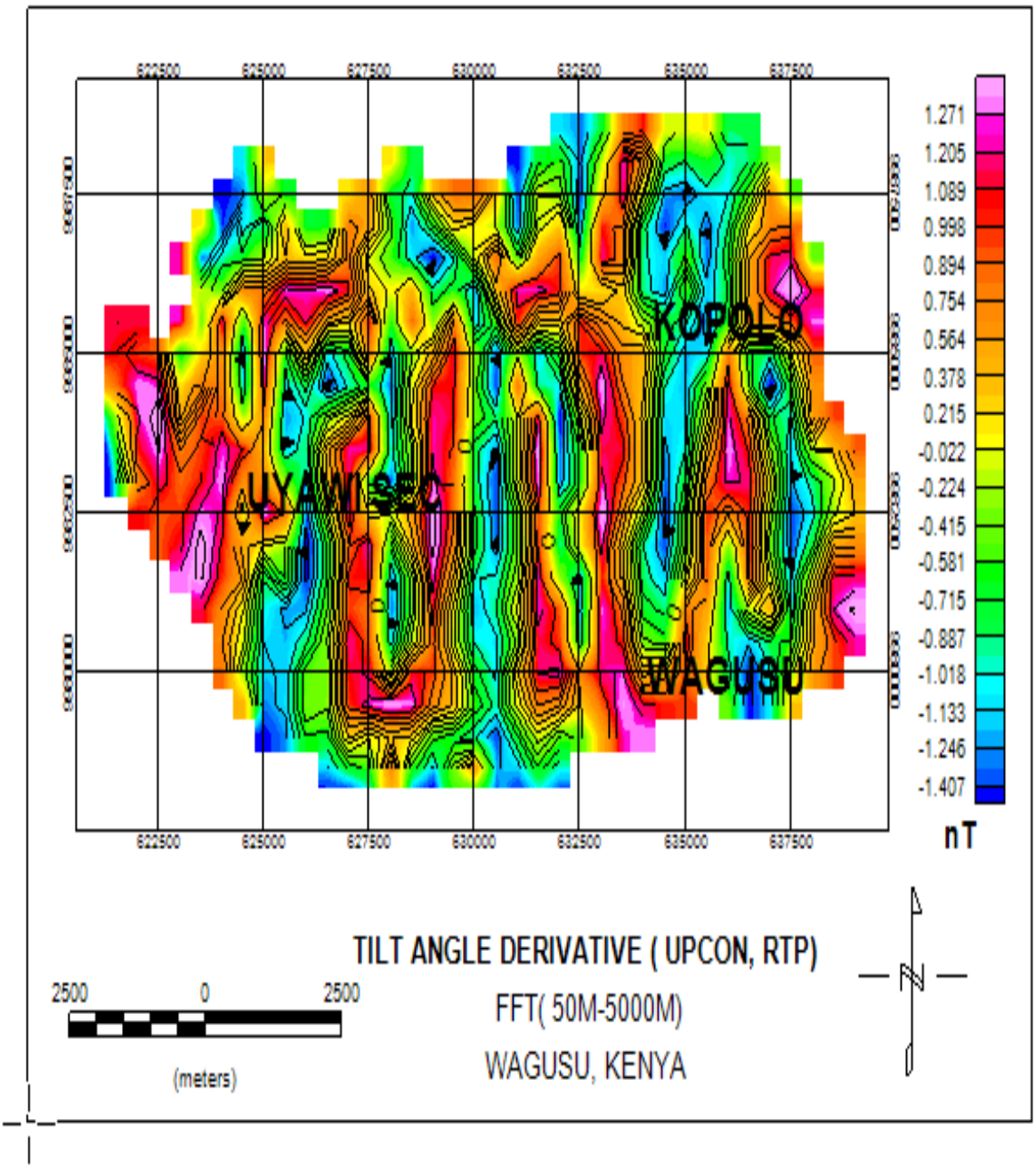

Figure 3.2: Tilt angle Derivative map for Magnetic residual anomaly (RTP) data

3.3 Power Spectral Analysis

Power Spectral Analysis examines signal spectra and analyzes their frequencies, signal quality, and power levels. The main advantage of power spectral analysis technique is its capability tto remove filter noise from a data by overlapping data while no information is lost during interpretation process. Such technique of spectral analysis provides rapid depth estimates from regularly-spaced digital data such as gravity or magnetic data (Specta and Grant, 1970). In order to achieve this, Wagusu area was treated as single block and a spectrum of radial average was produced since delineating structures bearing minerals entails mapping both deeper and shallow structures in the subsurface. This energy spectrum from radial averaging was used as a function of wavenumber only for band pass filter of 50m-5000m in depth. Depth was then estimated by averaging the energy for all directions for the same wavenumber. K, which was measured in cycles per unit distance.

The Nyquist wavenumber, N was the largest wavenumber sampled by the grid, which was the highest frequency possible to measure a fixed sample interval (Spector & Grant, 1970). Nyquist wave number is given by

$$N = \frac{1}{2Xi} = \frac{1}{2x0.5} = \quad 1 \qquad (3)$$

where i is the interval 500m of a sample.

Wave number K, ranges between 0 and 1, as shown in Figure 3.3. N used was 1 for the magnetic data. The axis of depth was in multiples of grid cells size that was 500 m for the study. The figure 3.3 represents power spectral peak between wave numbers 0.0004 cycles/meter and 0.0006 cycles/meter. It can be suggested that this contribution was from deep sources at approximated 4000 m in depth as shown on the depth estimate graph in Figure 3.3. The power spectral peak between wave numbers 0.0002 cycles/meter and 0.0004 cycles/meter revealed sources imaged at shallow approximated depth of 2150 m (Fig. 3.3)

Averaged depth for deep source = 4000 m

Averaged depth for shallow source = 2150 m

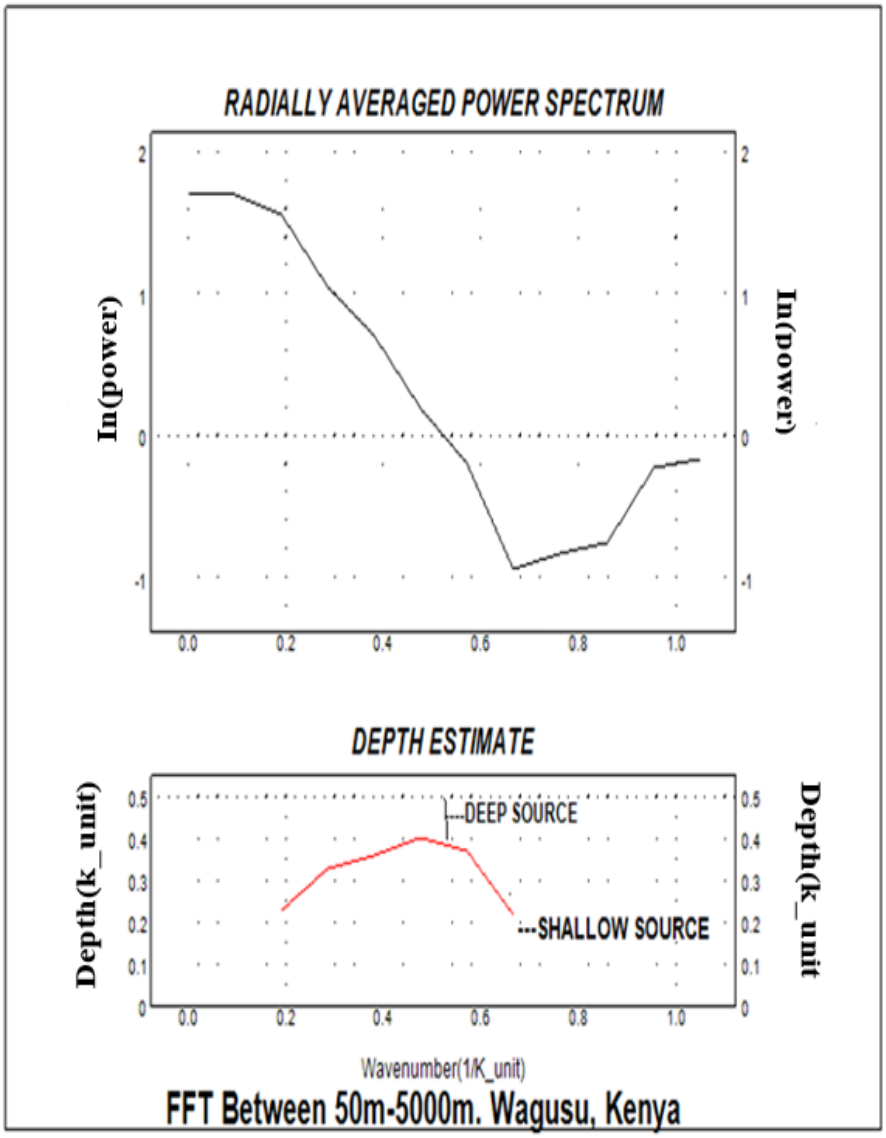

Figure 3.3: Power Spectral Analys for Magnetic residual (RTP) anomaly data

IV. Conclusions

Source depth contribution to band pass depth between 50 m- 5000 m was estimated for magnetic anomalies using power spectral analysis and tilt angle derivative techniques. From depth estimation graph (Fig. 3.3) of power spectral analysis, indicates depth estimates for high magnetic susceptibility causative anomalies of magnetic data. These source anomalies contribution to the energy spectra produced bottom depths between 2150 m and 4000 m. Tilt angle derivative also delineated source anomalies top depth range between 500m and 1300 m, so the mapped anomalies are seated between 500 m depth and 4000 m deep in the sub surface. In exploration fields for minerals, these causative anomalies are suggested to be structures for mineral deposits which are possibly structures bearing gold imaged at these depths. The variations in depth detection of the causative anomalies can be suggested to be due to intermittent cooling of hydrothermal mineral occurring in the igneous

and metamorphic rocks dominant regions. The anomalies could possibly be mafic or ultra mafic intrusive units containing magnetite or pyrrhotite or banded iron formation minerals in the metamorphic and unconsolidated rocks regions. The Analytic signal and tilt angle derivative maps also reveal contacts these causative anomalies. The contacts of anomalous magnetic intensity distribution on the study area are indicated by high magnetic intensity gradient and lie between the high amplitude magnetic anomaly and the low amplitude magnetic anomaly. Shear zones and faults are universally developed along these contrasting magnetic competencies. Along these contacts and along incompetent rocks, mineral deposits developed at these structural weaknesses. Competent rocks being enclosed in less competent favor fracturing and veining in the study area (Figs 3.1& 3.2). Common mineral associations of this kind include differentiated dolerite sills, tholeiitic basalts and banded iron formation. These fault lines or fractures or vein or contact zones could be path ways for hydrothermal mineral deposits such as gold seeping to near surface.

Acknowledgements
We are indebted to thank Jomo Kenyatta University of Agriculture and Technology for the invaluable assistance received from Physics and Geospatial Engineering departments. We also acknowledge Ministry of mining, Kenya for availing the data analysis software (Geosoft Oasis Montaj).

Conflict of Interests
We hereby declare that there is no conflict of interest attached to the publication of this paper whatsoever.

References

[1]. Abdelfettah, Y., Hinderer, J., Calvo, M., Dalmais, E., Maurer, V., & Genter, A. (2020). Using highly accurate land gravity and 3D geologic modeling to discriminate potential geothermal areas: Application to the Upper Rhine Graben, France. Geophysics, 85(2), 35-56. doi: 10.1190/geo2019-0042.1
[2]. Aziz, F., Miller, R., Giraldo, C., & Carigali, P. (2019). September 17th). Improving deep crustal structure depth interpretation by integrating 2D gravity-magnetic modeling and structural restoration: Offshore Borneo. Paper presented at the SEG International Exposition and 89th Annual Meeting, San Antonio, USA.
[3]. Barrachough, D.R., (1974). Spherical harmonic analysis of the geomagnetic field for eight epochs between 1600 and 1910. Geophys JR. Austr. Soc. 36 pp 497 - 513.
[4]. Beiki, M., and L. B. Pedersen, (2010). Eigenvector analysis of gravity gradient tensor to locate geologic bodies: Geophysics, 75, no. 6, I37–I49, doi: 10.1190/1.3484098.
[5]. Bell, R. and Dodson, M. H. (1981).The geochronology of Tanzania shield. Journal of Geology of Tanzania volume 89, 109-128.
[6]. Borg, G., Lyatuu, D. and Rammlmair, D., (1990). Genetic aspects of the Geita and Jubilee Reef Archean BIF-hosted gold deposits, Tanzania: Geologische Rundschau, v. 79, p. 355-371.
[7]. Bullard E. C., (1948). The secular change in the earth's magnetic field. Mon. Not. Roy. Astr. Soc. Geophys suppl. 5, pp 248-257.
[8]. Chenrai, P., (2010). Geophysical exploration at the Comet Gold Mine,Western Australia. M.S. thesis, Curtin University of Technology, Austalia.
[9]. Dawi, E. L., Tianyou, M. G., Hui, L., & Dapeny, L. (2004). Depth estimation of 2-D magnetic anomalous sources by using Euler deconvolution method. American Journal of Applied Sciences.
[10]. Dobrin, B.M. and Carl, S.H., (1988). Introduction to geophysical prospecting. MeGraw-Hill.Book Co. pp. 366 - 407.
[11]. Fedi, M., & Mastro, S. (2018). Bounded-Region Wavelet spectrum: a new tool for depth estimation of gravity and magnetic data. Paper presented at the SEG International Exposition and 88th annual Meeting, Napoli, Italy.
[12]. Florio, F., M. Fedi, and R. Pasteka, (2006). On the application of euler deconvolution to the analytic signal: Geophysics, 71, no. 6, L87–L93, doi:10.1190/1.2360204.
[13]. Georgsson. (2009). Geophysical methods used in geothermal exploration. Paper presented at the Short Course IV on Exploration for Geothermal Resources, organized by UNU-GTP, KenGen and GDC, Lake Naivasha, Kenya.
[14]. Geosoft (Oasis Montaj) program, Geosoft mapping and Application system. Inc. Suit 500, Richmond St. West Toronto. ON Canada. 2007.
[15]. Goldfarb R.J., Baker T., Dube B., Groves D.I., Hart C. J.R, Gosselin P., (2005). Distribution, Character. And Genesis of Gold Deposits in Metamorphic Teranes, in Economic Geology. 100th Anniversary Volume, 407-450.
[16]. Haidarian Shahri, M. R., Karimpour, M. H. and Malekzadeh, A., (2007). Pyrrhotite – a clue to gold at portion of the Hired gold mineralization, eastern Iran, GSA annual meeting, 28-31.
[17]. Holden, E., J. C. Wong, P. Kovesi, D. Wedge et al. (2012). Identifying Structural Complexity in Aeromagnetic Data: An Image Analysis Approach to Greenfields Gold Exploration, Ore Geol. Rev., 46, 47-59, doi:10.1016/j. oregeorev.2011.11.002.
[18]. Holden, E., P. Kovesi, M. Dentith, D. Wedge et al. (2010). Detection of regions of Structural Complexity within Aeromagnetic Data using Image Analysis, 25th International Conference of Image and Vision Computing New Zealand, 1-8, doi:10.1109/IVCNZ.2010.6148856.
[19]. Hong, L., Jianbao, Y., Hui, L., Pengfei, X., & Sinopec Geophysical Research Institute, C. (2017). Gravity and aeromagnetic data interpretation of the Xiongxian geothermal system, China. Paper presented at the SEG International Exposition and 87th Annual Meeting.
[20]. Ichangi D.W. (1993). Lithostratigraphic setting of mineralization in the Migori segment of the Nyanza Greenstone Belt, Kenya. In: Proceedings of the fifth conference of the geology of Kenya. Nairobi, Kenya.
[21]. Karimpour, M. H., Malekzadeh, A., Haidarian Shahri, M. R., and Askari, A., (2007), Geology, Mineralogy, and Geochemistry of Heired gold exploration, Khorasane Jnoobi, Proceeding of the 14th Symposium of Crystallography and Mineralogy of Iran, 278-284.
[22]. Kearey P., Michael B., and Ian H. (2002). An Introduction to Geophysical Exploration. 3rd edition. London: Blackwell Scientific publications.
[23]. Kitson, A.E. (1934). Geological reconnaissance in Kavirondo and other District of Kenya. Final report
[24]. Konadu, B.A., Isaac, D., & Kwaku, T.K. (2018). Integrating gravity and magnetic field data to delineate structurally controlled gold mineralization in Sefwi Belt of Ghana. Journal of Geophysics and Engineering 15(2018) 11971203(7pp).

[25]. Lowes, F. J., (1984). The geomagnetic dynamo elementary energetics and thermodynamics. Geophysical surveys 7, pp. 91 - 105.
[26]. Lowrie, W. (2007). Fundamentals of Geophysics (Second ed.). NewYork: Cambridge University Press, pp. 77 – 95.
[27]. Mariita, N. (1995). Exploration for Geothermal Energy in Kenya – A Historical Perspective. Geothermal research report. Japan: Kyushu University.
[28]. Mariita, N. (2011). Application of geophysical methods to geothermal energy exploration in Kenya. Paper presented at the Short Course VI on Exploration for Geothermal Resources, UNU GTP, GDC and KenGen, Lake Bogoria and Lake Naivasha, Kenya. **Error! Bookmark not defined.**
[29]. Miller, H. G., & Singh, V. (1994). Potential field tilt—a new concept for location of potential field sources. Journal of Applied Geophysics, 32(2–3), 213–217.
[30]. Ndombi, J. M. (1981). The structure of the shallow crust beneath the Olkaria geothermal field, Kenya, deduced from gravity studies. J. Volcanol. Geotherm. Res, 9(237- 251).
[31]. Odek, A., Githiri, J., and Korowe, M. (2021). Demarcating productive parts of Migori Green Stone belt using Edge Detection Technique, Journal of Geology and Geophysics Vol. 1.
[32]. Petrova, G.N., Bobrov, V.N., and Pudovkin, M.I., (1980). Geomagnetism. pp. 1-23.
[33]. Pipan, M. (2009). Remote sensing and geophysical methods for geothermal exploration. Presented at the School on Geothermics, organized by ICTP, ICS-UNIDO and IAEA, Trieste, Italy.
[34]. Pulfrey, W., (1946). Geological Survey of Maragoli, Northern Kavirondo. Report NO.9, Geology survey of Kenya.
[35]. Reid, A. B., J. M. Allsop, H. Grancer, A. J. Millet, and I.W. Somerton, (1990). Magnetic interpretation in three dimensions using euler deconvolution: Geophysics, 55, 80–91, doi: 10.1190/1.1442774
[36]. Robert, F, Poulsen, K.H., and Dube, B., (1997). Gold deposits and their geological classification, in A.G. Gubins, ed, Proceedings of Exploration 97; Fouth Decennial International Conference on Mineral Exploration, 209-220
[37]. Salem A., Williams S., Fairhead D., Smith R., Ravat D. (2008). Interpretation of magnetic data using tilt angle derivatives. Geophysics, 73, L1-L10.
[38]. Salimo, L., (2013). Gold mineralization at Masumbi AU-CU prospect, West Kenya: Implication for gold exploration in the Archean Ndori Greenstone Belt of Kenya.
[39]. Shackleton, R.M., (1951). A contribution to the geology of the Kavirondon Rift Valley: Quarterly Journal of the Geological Society, v. 106, pp. 345-392.
[40]. Simmons, S.F., White, N.C and John, D.A., (2005). Geological characteristics of epithermal precious and base metal deposits, in Economic Geology. 100th Anniversary Volume, 485-522.
[41]. Spector, A., & Grant, F. S. (1970). Statistical models for interpreting aeromagnetic data. Geophysics, 35(2), 293-302.
[42]. Telford, W. M., Geldart, L. P., & Sheriff, R. E. (1990). Applied Geophysics. Cambridge: Cambridge University Press.
[43]. Verhoogen,J., (1973). Thermal regime of the earth's core. Phys. Earth planet Int. P 7. pp. 47 - 58.
[44]. Warega, J. A., Githiri, J., & Ambusso, W. (2020). "Geothermal prospecting of Olkaria Dome Areas in Naivasha, Nakuru County-Kenya using gravity method." Journal of Earth and Environmental sciences Vol 4. Pg 3 issue 01 ISSN 2577 – 0640.
[45]. Warega, J.A., K'orowe Maurice., Githiri, J., & Munyithya, J. (2025). "Application of high-resolution gravity data for depth and edge detection of Gold bearing bodies in Central Sakwa Bondo Siaya County, Kenya" Journal of Emerging Technologies and Innovative Research. Vol 12. Pg e215-e226 issue 8 ISSN 2340-5162.
[46]. Wright, C., Barton,T., Goleby, B.R., Spence, A.G. & Pester, D. (1981). The interpretation of expanding spread profiles: examples from central and eastern Australia. Tectonophysics, 173, 73–82.
[47]. Yehuwalashet, E., & Malehmir, A. (2018). Gravity and magnetic survey, modeling and interpretation in the Blötberget iron-oxide mining area of central Sweden. Paper presented at the SEG International Exposition and 88th annual Meeting.
[48]. Yukutane, T. and Tachinaka, H., (1968). The non-dipole part of the earth's magnetic field. Bull. Earth quake Res. Insti. 46, pp 1027 – 1062.